Proceedings World Geothermal Congress 2020+1
Reykjavik, Iceland, April - October 2021

An Analysis of 40 Years of Subsidence due to Geothermal Production from the Svartsengi-Eldvörp Geothermal System in SW Iceland

Melissa Anne De Freitas[1,3], Guðni Axelsson[2] and Páll Einarsson[3]

1) Energy Unit, Kingstown VC0100, St. Vincent & the Grenadines 2) Iceland GeoSurvey (ÍSOR), Grensásvegur 9, IS-108 Reykjavík, Iceland 3) Institute of Earth Sciences, University of Iceland

mad22@hi.is; melissa.defreitas@gov.vc

Keywords: Reykjanes Peninsula, Svartsengi, Eldvörp, TOUGH2, iTOUGH2, subsidence, reservoir model, numerical modelling

ABSTRACT

The Svartsengi-Eldvörp geothermal system is a high-temperature system situated within the Reykjanes Peninsula oblique rift in south-west Iceland that bounds the North American and Eurasian tectonic plates. Based on its geological location, Svartsengi is prone to many complex crustal deformation processes. Extensive regional ground subsidence ranging from 7 to 14 mm/year was observed from 1975 to 2015 along the Reykjanes Peninsula, with maximum changes in elevation detected within the main production field at Svartsengi. There have been numerous studies undertaken that have been aimed at identifying and isolating the various signals that contribute to this observed subsidence, with more recent studies proposing a natural subsidence velocity of 6 mm/year along the central volcanic rift of the Reykjanes Peninsula. This paper contributes to previous deformation studies conducted at Svartsengi through the development of a TOUGH2 numerical model of the Svartsengi geothermal system. The model is calibrated against initial thermodynamic conditions, the average annual mass extraction and reinjection rates during 40 years of production from 1975 to 2015, and the resulting reservoir response. One-dimensional subsidence modelling was performed with the model, using a newly developed subsidence module in iTOUGH2. Modelled results revealed an average subsidence velocity of 3-4 mm/year due to geothermal activity at Svartsengi. Despite only considering one-dimensional subsidence and coupled with the natural subsidence value previously determined, the model accurately represents the total subsidence observed at Svartsengi. This numerical model is therefore capable of predicting subsidence rates due to future geothermal utilization at the Svartsengi and Eldvörp.

1. INTRODUCTION

Iceland lies astride the Mid-Atlantic Ridge, bounding the rifting and transform segments that divides the North- American and Eurasian tectonic plates. The Mid-Atlantic Ridge is defined by a narrow zone of deformation observed, with geological and geodetic observations revealing a plate divergence rate of approximately 17-18 mm/year in Iceland (DeMets, et al. 1994). In south-west Iceland, the Reykjanes Ridge (RR) segment of the Mid-Atlantic Ridge comes onshore at the Reykjanes Peninsula (RP), extending from there with an azimuth trend of 70° along the entire peninsula (Einarsson 2008). The location of the Reykjanes Peninsula is shown in Figure 1. The westward motion of the ridge with respect to the proximity of the deep mantle plume located under Vatnajökull, illustrated in Figure 1A. (Wolfe, et al. 1997), has resulted in an offset from the plate boundary.

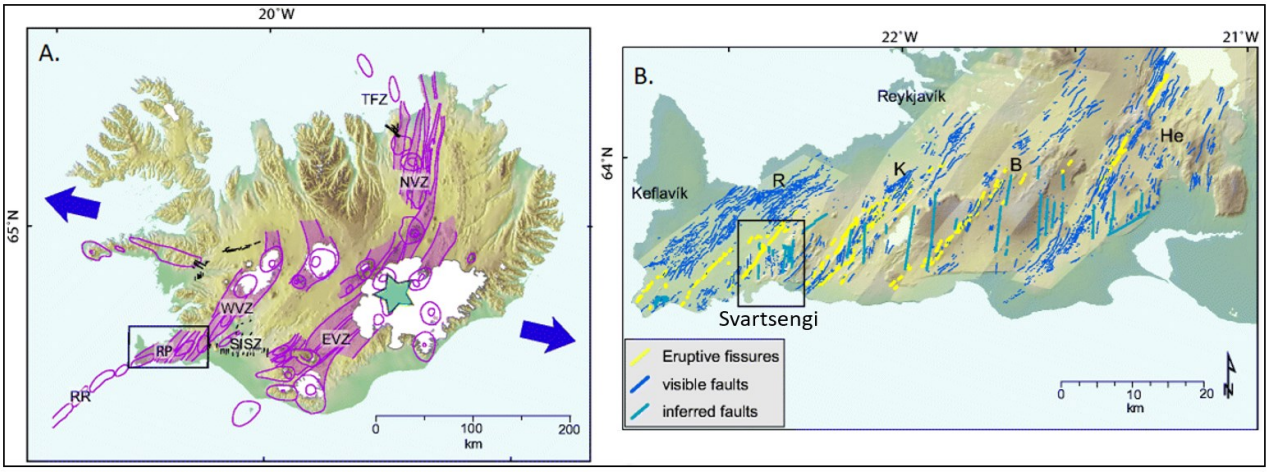

Figure 1: (A) Tectonic map of Iceland (Einarsson and Sæmundsson 1987) modified by Clifton and Kattenhorn (2006) showing ridge segments. The centre of mantle plume is indicated by the green star. The shaded purple areas denote volcanic systems, while the white areas represents the glaciers. Dark blue arrows indicate the direction of plate motion. (B). Map of Reykjanes Peninsula showing main tectonic features and fissure swarms (Clifton and Kattenhorn 2006)

Iceland's geographical and geological setting has resulted in it being a very tectonically and volcanically active area, with an extensive geothermal potential. Svartsengi, being located on the Reykjanes Peninsula, is prone to many complex crustal deformation processes, with active tectonism, volcanism and seismicity long since been identified as major contributors to ground deformation occurring in Svartsengi, with subsidence velocities within the range of 7-14 mm/year observed during 1975 to 2015 (Eysteinsson 2000; Magnússon 2009; 2013; 2015). Subsidence in the Reykjanes Peninsula has been extensively monitored, with

numerous studies done to attempt to isolate the various signals that contribute to ground deformation. A combined analysis of a variety of geodetic studies and lithological logs (Vadon and Sigmundsson, 1997; Fridleifsson and Richter, 2010) have proposed a background subsidence rate of approximately 6 mm/year along the central rift zone of the Reykjanes Peninsula. The commencement of geothermal production at Svartsengi saw the formation of a large subsidence bowl around Svartsengi and Eldvörp within the first few years, with over 0.36 m of subsidence observed between 1975 and 2014 over the main production field at Svartsengi (Magnússon, 2015). A direct relationship observed between the pressure drawdown and subsidence led Eysteinsson (2000) to infer that geothermal production at Svartsengi was one of the major contributors to the vertical deformation observed during this period.

Numerical modelling plays a vital role in comprehending the nature of geothermal systems and is one of the most powerful tools of geothermal reservoir engineering, utilized globally to simulate the production response of geothermal reservoirs to a variety of scenarios. Though used extensively for geothermal resource assessment, geothermal reservoir models have recently begun to include the resultant subsidence due to geothermal production as an additional model calibration factor. Numerous numerical production models have been developed for Svartsengi throughout the last 40 years of production (e.g. Bödvarsson, 1988; Björnsson, 1999; Ketilsson, 2007), however these have not directly incorporated the observed subsidence due to geothermal production. A recent example of this was done for the Wairakei geothermal system in New Zealand, which accurately reproduced the subsidence observed during 50 years of geothermal production (Koros, et al. 2016), leading the authors to conclude that these models are valuable tools in forecasting subsidence rates due to geothermal production.

This research project was therefore aimed at isolating the geothermal signal of the total subsidence observed in Svartsengi through the creation of a TOUGH2 numerical reservoir model, calibrated against the production response based on 40 years of geothermal exploitation from 1975 to 2015. The resultant subsidence was then calculated from the TOUGH2 production model created, employing the newly developed one-dimensional subsidence module in iTOUGH2 (Finsterle 2018a and 2018b). These results are presented in Chapter 5.

2. SVARTSENGI GEOTHERMAL SYSTEM

2.1 Subsurface Geology of the Svartsengi Geothermal Field

The Svartsengi field lies within a basaltic lava field at low elevations between 20-30 m a.s.l. surrounded by low hyaloclastite mountains. Eldvörp is located approximately six kilometres WSW from the Svartsengi production field (Figure 2A). Though previously treated as separate systems, numerous studies have since proven a clear connection between Svartsengi and Eldvörp.

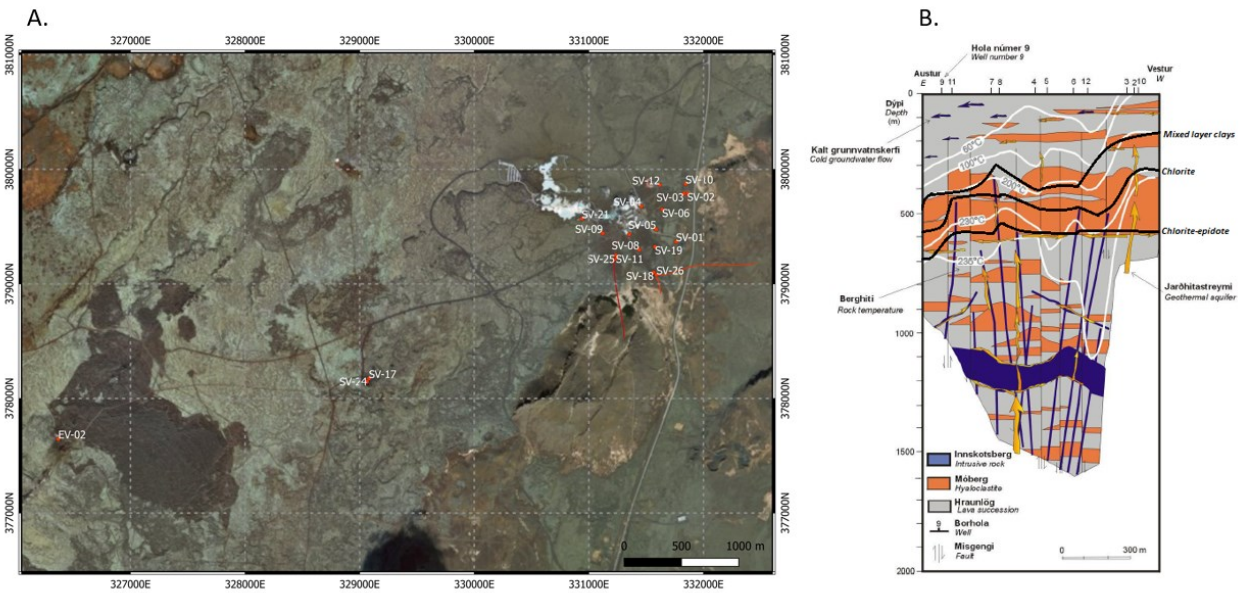

Figure 2: (A) Map revealing the location of bore-holes within the Svartsengi Geothermal System. Directionally drilled wells are indicated in red and (B) Geological cross section, modified from Franzson (1990).

There are 25 wells presently drilled into the main Svartsengi production field, and one in Eldvörp attaining depths from a few hundred metres to just over 2000 m b.s.l. An ENE-WSW trending cross section of the first 12 wells drilled into the reservoir is presented in Figure 2B, summarising the main alteration features, as well as the relationship between the alteration mineralogy found in wells 2- 10 and their formation temperatures. The elevation of the mixed-layer clay and chlorite zones observed in the east corresponds to the reservoir's expanding steam zone. Hyaloclastite layers of thickness 100 m are scattered throughout the profile, with an exception of the layer located between 300- 600 m which is observed in most of the deeper wells, acting as a caprock to the hydrothermal system. Dislocations of hyaloclastite boundaries observed in Figure 2B indicates faults dissecting the strata. Intrusives, ranging from dykes to sills (Franzson 2017) are observed below 800 m depth. The vast number of vertical intrusives and fractures illustrated in Figure 2B have resulted in a high vertical permeability distribution throughout the field. A hydrological model of the Svartsengi area presented by Kjaran et al. (1979 and 1980) found the total average permeability of the reservoir to be in the range of 100-150 mDarcy.

2.2 Resistivity Structure of the Svartsengi Geothermal Field

Early DC resistivity surveys conducted along the western Reykjanes Peninsula revealed a shallow, low resistivity zone along the Reykjanes plate boundary (Georgsson 1981). A Transient Electromagnetic (TEM) later conducted revealed a common reservoir with clearly defined boundaries spanning an area of 30 km^2 at 1000 m b.s.l, extending from Eldvörp to Svartsengi shown in Figure 3A (Karlsdóttir 1998). This reveals a resistivity profile synonymous with that of high-temperature geothermal field. In these systems, the resistivity is relatively high in cold unaltered rocks outside the reservoir. A low-resistivity cap is observed between 300 – 600 m b.s.l on the outer, upper margins of the reservoirs, underlain by a highly resistive core- indicative of the location of the geothermal reservoir.

A vast magnetotelluric (MT) survey later carried out (Karlsdottir and Vilhjálmsson 2015) further confirmed the resistivity profile of the earlier TEM model by Karlsdóttir (1998). Figure 3B reveals three upflow zones, observed as instances of up-doming of the high resistivity core into the overlying low resistivity clay cap layer. These upflow zones correspond to the locations of both the Svartsengi well field, the Eldvörp fissure swarm; and another located between Svartsengi and Eldvörp at approximately 4 km SW of the Svartsengi well field.

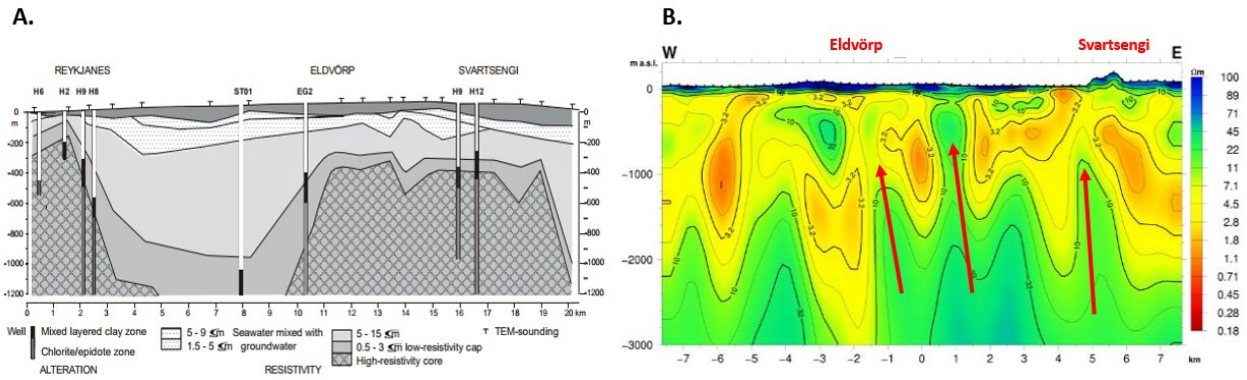

Figure 3: (A) ESE-WNW trending TEM cross section along the outer Reykjanes Peninsula (Karlsdóttir 1998) and (B) Resistivity cross section through Svartsengi down to 3000 metres depth b.s.l., modified from Karlsdóttir and Vilhjálmsson (2015), with arrows pointing towards upflow areas.

2.3 Conceptual Model

Formation temperatures (Figure 4A) were calculated through the analysis of numerous temperature logs (Björnsson and Steingrímsson 1991). The determination of the formation temperature reveal pertinent information on the physical characteristics of the reservoir. There are two observable zones within the reservoir. Wells SV-02, SV-03 and SV-10 lie on the boiling point curve, and are thus producing from the steam zone. Although they are not included in the analysis for this paper, wells SV-14, SV-16, SV-20, SV-22 and SV-23 are also producing from the shallow steam zone while the remaining wells are producing from the liquid-dominated reservoir, with uniformed temperatures of 240°C below 900 m depth within the main production zone. In these wells, the temperature remains relatively constant with depth, which is suggestive of a highly permeable reservoir with good convective mixing (Grant and Bixley 2011).This analysis led to the subsequent development of a conceptual model (Figure 4B) for the entire Svartsengi geothermal field (Björnsson and Steingrímsson 1991).

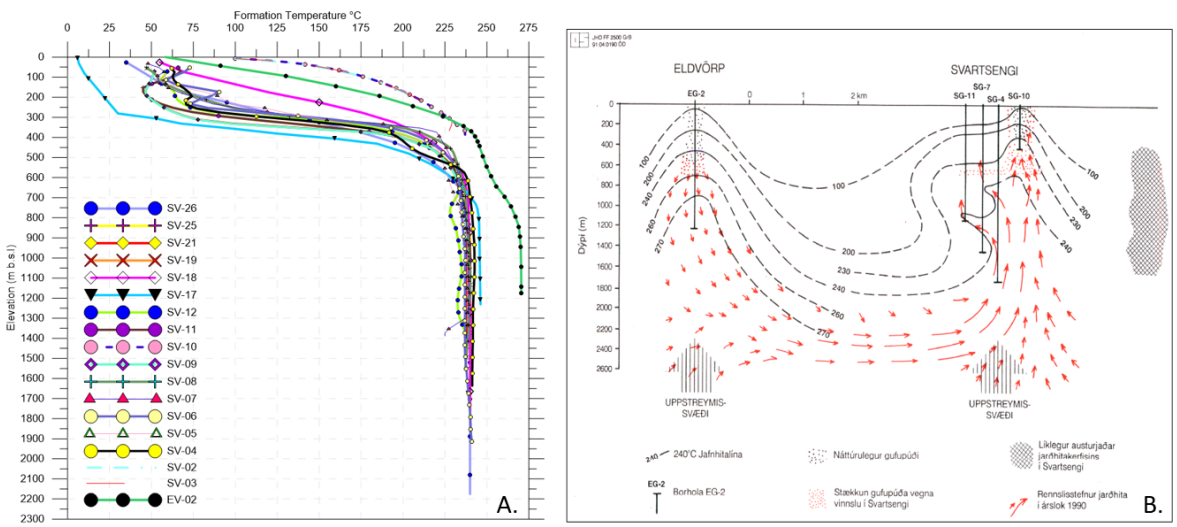

Figure 4: (A) Formation temperature profiles for wells drilled into the Eldvörp - Svartsengi geothermal area, and (B) Conceptual model developed through analysis of Formation temperature profiles (Björnsson and Steingrímsson, 1991)

Based on observations, the location of three aquifer systems within the Svartsengi field were incorporated in Figure 4B; a warm groundwater system located between 30-300 m; the main liquid dominated reservoir below 600 m b.s.l, and a two-phase chimney in

the north east part of the field. Further analysis revealed a temperature anomaly which was interpreted as the main upflow zone to the Svartsengi well field, feeding the permeable horizontal intrusive layers, as well as the steam chimney of the two-phase system. Two upflow zones were included in Figure 4B, the other being an upflow along the Eldvörp fissure swarm earlier proposed by Franzson (1987).

3. PRODUCTION AND RESERVOIR RESPONSE

3.1 Production and Reinjection History

Commercial production at Svartsengi commenced in October 1976. Figure 5 gives the annual average production and reinjection at Svartsengi from 1976 to 2016, as well as the observed pressure drawdown in wells EV-02, SV-08, SV-09, SV-11, SV-12 and SV-19. There was a step-wise increase in production from 1976 to 1982, from 0.36 to 7.73 million tons per year, equivalent to 11.43 and 245 kg/s average production, respectively. During the following years, from 1983 to 1999, the average annual production gradually increased, fluctuating between the range of 7.21 to 10 million tons, equivalent to 220 and 300 kg/s average production, respectively. From 2000-2006, the average production declined, however has increased since 2006. By 2016, the total annual production in was 14.4 million tons, equivalent to 456 kg/s on average. This represents a 6% decrease from 2014, when production was 15.4 million tons, equivalent to 488 kg/s - the maximum production that has occurred at Svartsengi during the period 1976-2016.

The first reinjection well, SV-12, was drilled in 1982, to a depth of 1488 m b.s.l. and was used for reinjection during 1984-1988. It was drilled based on two criteria: it was drilled within the confirmed reservoir; and if reinjection into the well was not feasible, the well would then be utilised for production (Guðmundsson 1983).When reinjection into SV-12 was discontinued, reinjection into SV-05 continued until 1990. From 1993, fluid was intermittently reinjected into SV-06 until 2000. These wells however are all located in the main production field at Svartsengi, and if reinjection were to continue at the same flow rates, though it may have offered significant pressure support, rapid cooling would have occurred (Þóhallsson, et al. 2004). SV-17 therefore was drilled about 2.3 km away from the main well field with the main objective of providing adequate pressure support to the system without the risk of cooling. Reinjection commenced here in 2000, with another reinjection well – SV-24 later drilled on the same platform as SV-17.

Figure 5B shows a rapid pressure decline in Eldvörp and Svartsengi before the commencement of large scale reinjection in 2000 of approximately 22 bars and 15 bars respectively. The total drawdown in Svartsengi since 1975 is approximately 34 bars. The pressure drawdown in Eldvörp at 1100 m depth follows the same trend as the decline in Svartsengi, with pressure in both fields reacting strongly to reinjection in Svartsengi. This observed pressure connection between Svartsengi and Eldvörp corroborates the hydrological connection between the two areas and therefore confirms that Eldvörp is a part of the Svartsengi geothermal field (Guðmundsdóttir 2016).

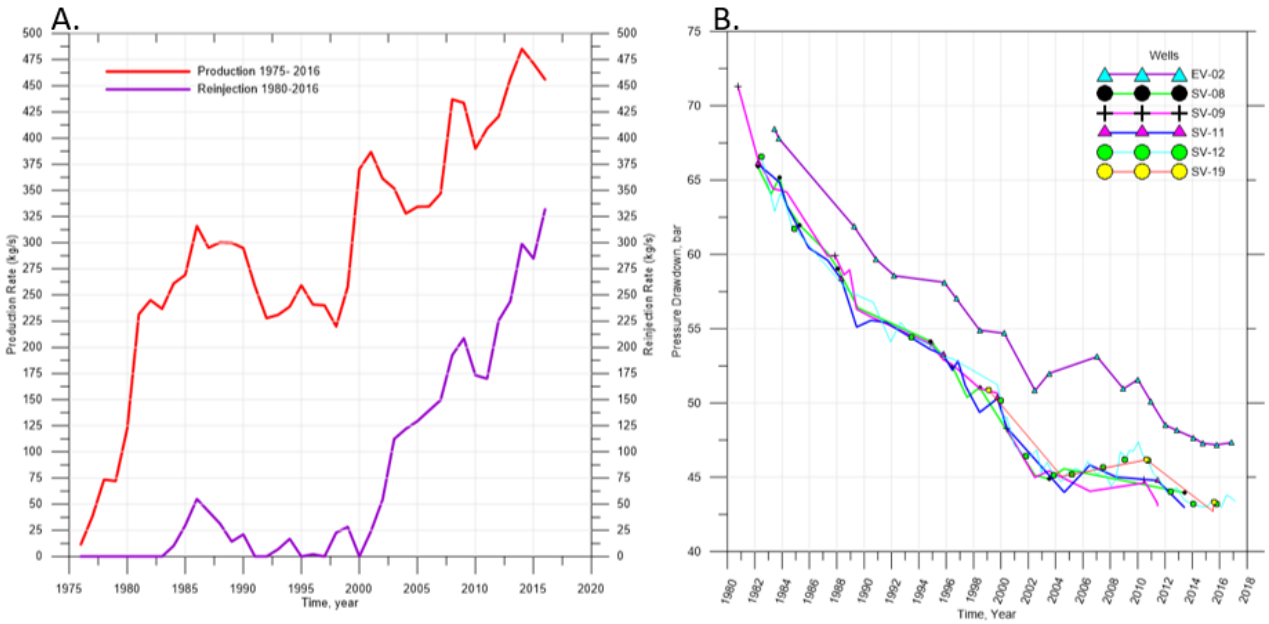

Figure 5: (A) Production and reinjection history at Svartsengi for the period 1975-2016 and (B) Pressure decline (1980-2017) at 900 m b.s.l. in SV-08, SV-09, SV-11, SV-12, SV-19 and at 1100 m b.s.l. in EV-02.

3.2 Subsidence (1976-2016)

Ground Deformation at the Reykjanes Peninsula is due to a combination of different factors such as tectonism, seismic activity, geothermal activity, load variation and volcanism with many recent attempts made to isolate the different signals that contribute to the total observed deformation (Vadon and Sigmundsson, 1997; Hreinsdóttir et al., 2001; Árnadóttir et al., 2004; Keiding et al., 2008 and 2010; Receveur 2018). InSAR analysis conducted by Vadon and Sigmundsson (1997) estimated a long term natural subsidence of approximately 6.5 mm/year within the central part of the rift zone. More recently, lithological logs obtained from the Iceland Deep Drilling Project (IDDP) at Reykjanes revealed the presence of shallow marine deposits at 500 m depths. Based on the analysis of surrounding lithology, Fridleifsson and Richter (2010) estimated a long term average background subsidence velocity of 6.0 mm/year throughout the past 500,000 years, consistent with that of Vadon and Sigmundsson (1997).

In an attempt to monitor the resulting ground deformation due to geothermal production, the subsidence in the Reykjanes Peninsula has been extensively monitored. This was done initially by levelling and gravity measurements (Eysteinssom, 1993; 2000), and later on additionally by GPS (Magnússon, 2009; 2013; 2015) and Interferometric Synthetic-Aperture Radar (InSAR) analysis (Vadon and Sigmundsson, 1997; Keiding et al., 2008; Receveur, 2018). Extensive geodetic levelling conducted between 1975 to 1992 (Eysteinsson, 1993) revealed a vast, elongated subsidence bowl spanning an area of over 100 km^2, with maximum subsidence centred on the Svartsengi well-field (Figure 6).

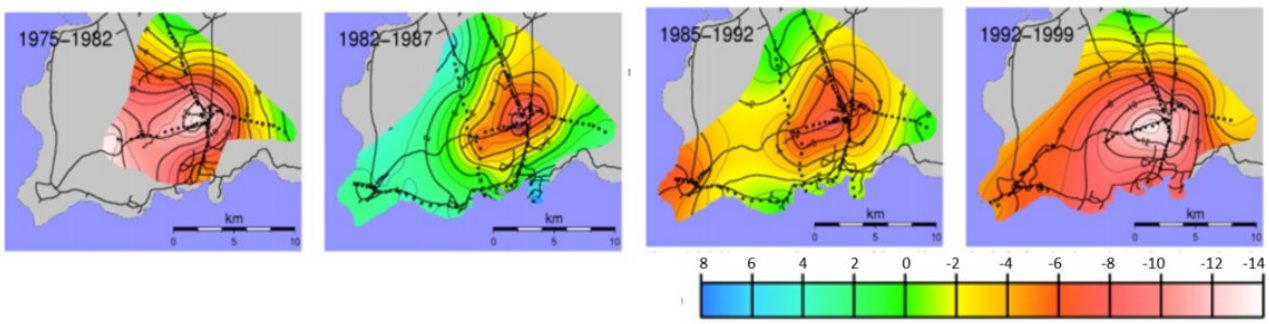

Figure 6: Average subsidence rate in the Reykjanes Peninsula from 1975-1999 (Eysteinsson, 2000).

The average rate of subsidence in Svartsengi during the first 7 years of production was 14 mm/year, with the maximum located directly at the centre of the wellfield, reducing to 7-8 mm/year from 1982 to 1992. The average subsidence increased during 1992-1999 to 14 mm/year, decreasing again during 1999-2004 (Figure 7) after the commencement of large scale reinjection to approximately 6 mm/year (Magnússon, 2009). From 2004-2008, there was an increase to 12 mm/year (Magnússon, 2009) corresponding to an increase in production during this period. There was a minor decrease in the subsidence rate in Svartsengi from 2008 to 2014, to approximately 10 mm/year (Magnússon, 2015). This represents an average rate of 10 mm/year during 1999-2014. This decrease in subsidence may be explained by the increase in reinjection during this period (Figure 5). A more recent interferometric analysis of InSAR data from 2015-2017 (Receveur, 2018) reveals subsidence rates at Svartsengi of approximately 8-10 mm/year during this period (Figure 27), analogous to results during the period 2010-2014.

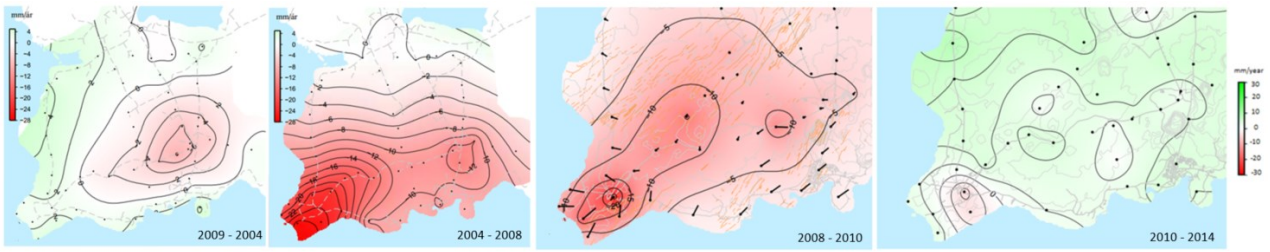

Figure 7: Subsidence of the Reykjanes Peninsula inferred from GPS surveys from 1999-2014 (Magnússon, 2009; 2013; 2015).

4. DEVELOPMENT OF NUMERICAL MODEL FOR THE SVARTSENGI GEOTHERMAL SYSTEM

4.1 The Natural State

A simple numerical model for the entire Svartsengi geothermal system was developed for this project. A Voronoi grid extending over total horizontal area of 468 km^2, from sea level to 2550 m b.s.l. was produced. It is divided vertically into 13 layers of varying thickness, depicted in Figure 8, with thinner layers defined closer to the surface and base (Layer A and M respectively), and thicker layers modelled deeper into the liquid-dominated reservoir (Layers E-J). The grid is discretised horizontally with rather course elements around the perimeter of the wellfield, and finer elements within the wellfield where more precision is required. Dirichlet boundary conditions were employed to the top and bottom layers and around the lateral edges of the grid to control the initial conditions of the reservoir. A constant geothermal gradient of 100 °C/km was fixed over the entire grid, with a surface temperature of 3 °C and corresponding hydrostatic pressure gradient. At the midpoint of the inactive and impermeable surface layer (i.e. at 100 m b.s.l.), the temperature is kept constant at 13 °C, while within the boundary, the temperature increases with depth according to the geothermal gradient, remaining constant with time- therefore permitting the inflow of cooler fluids according to pressure decline.

A low permeability caprock was modelled in Layers B and C, with the reservoir extending from Layer D to the base. Three upflow zones were included in the model. Source A represents the upflow along the Eldvörp fissure (Franzson, 1987), while C represents the upflow to the main production area (Björnsson and Steingrímsson 1991). The third source (B), between Eldvörp and Svartsengi was included due to the observations from the MT profile in Figure 3B (Karlsdóttir and Vilhjálmsson, 2015). These upflow areas, A, B and C are modelled as highly permeable vertical fractures with assigned rocks FRAC1, FRAC2 and FRAC3 respectively, surrounded by reservoir rocks of lower permeabilities. A schematic of the initial rock distribution throughout the model is presented in Figure 9.

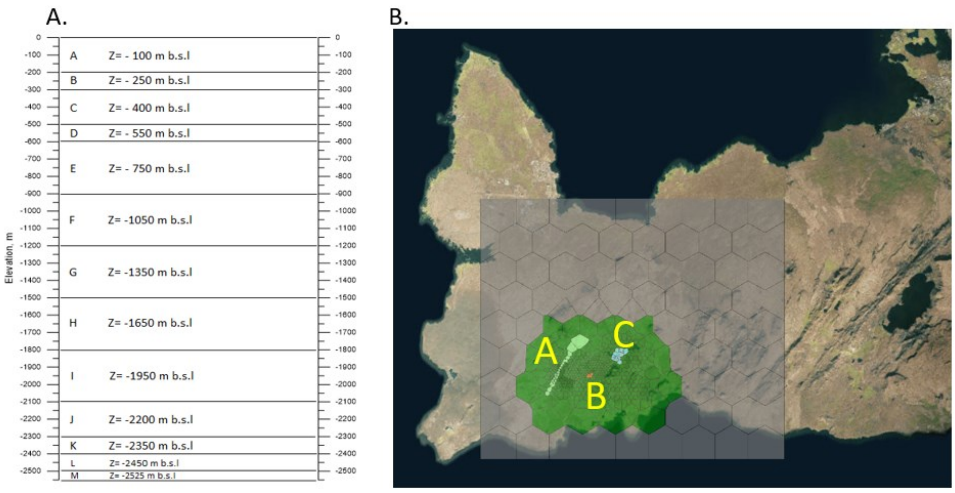

Figure 8: (A) Vertical profile of the Svartsengi model, showing layers A-M, with (B) location of upflow zones, A, B and C modelled in Layer L at -2450 m b.s.l.

Constant physical reservoir properties utilised in previous models (Bödvarsson, 1988; Ketilson, 2007) together with further rock coefficients utilised by Ketilsson (2007) were imported into TOUGH2, and using Equation of State 1 (EOS1), the conditions were simulated forward in time for 100,000 years. PyTOUGH (Croucher 2017) was used to extract output variables from the TOUGH2 output file. The modelled temperature profiles were compared the formation temperature profile. Rock parameters, fluid enthalpy and flow rates were manually adjusted in an attempt replicate the observed formation temperature profiles.

4.2 Production History Matching

The pressure drawdown observed in Figure 5 between Svartsengi and Eldvörp suggests a strong pressure connection with a high permeability zone extending from Svartsengi to Eldvörp. The model was therefore altered, with a horizontal permeability zone increasing from the inactive boundary towards the centre of the grid, where k_1>k2>k3>k4>k5 (Figure 9B). A highly permeable rock material connects Svartsengi to Eldvörp, which should establish a connection between the two points.

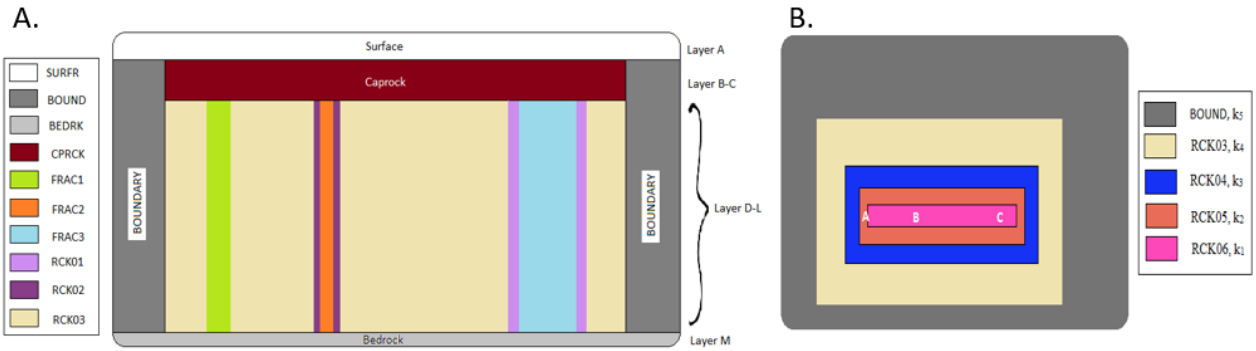

Figure 9: A schematic of the initial vertical (A) and horizontal (B) rock distribution within the Svartsengi system.

The model assumes three feed zones:

1. Layer C (300-500 m b.s.l.) – used to represent the conditions of the steam zone.
2. Layer F (900-1200 m b.s.l.) – accounting for production and reinjection in all other wells within the main well field.
3. Layer D (500-600 m b.s.l) – simulating reinjection in wells SV-17 and SV-24.

Production was simulated by distributing the average annual production among production wells in the main wellfield. Reinjected fluid of temperature 98°C, which corresponds to an enthalpy of 3.98 x 105 J/kg, was injected in wells SV-05, SV-06, SV-12, SV-17 and SV-24 according to the reinjection history previously described.

These parameters were then input into TOUGH2 and simulated for 41 years (i.e. from 1975 to 2016). PyTOUGH was used to extract and visualise the modelled pressure drawdown in Layer F for wells EV-02, SV-08, SV-09, SV-11, SV-12 and SV-19. These were compared to the values observed during 1980-2017 in Figure 5B.

5. RESULTS AND DISCUSSION

There are 26 wells currently drilled into the Svartsengi-Eldvörp system. Usually, a well-by-well approach is taken where each well is assigned one specific element, and the element is calibrated according to the observed conditions in that well. In this study, however, wells located close together were grouped and modelled as a single well. This was done to maintain a certain simplicity in the model, justified by the fact that temperature conditions in the main well field are quite uniform. Additionally, the main purpose of the study was not an accurate and detailed replication of well-by-well variability, but rather the overall effect of mass extraction on reservoir pressure and subsidence.

5.1 Temperature Model

The model is heated up from below by a constant temperature boundary. A uniformed background temperature of 255 °C was initially applied to Layer M (base) of the model, however, during the calibration process, a higher temperature of 280 °C was applied along the Eldvörp fissure in layer M to reflect the more elevated temperatures observed in well EV-02. In achieving steady state;

- A total of 55 kg/s of fluid, with an enthalpy of 1236 kJ/kg was injected into the highly permeable elements that made up Source A along the Eldvörp fissure system.
- A total of 40 kg/s of fluid, with enthalpy 1117 kJ/kg was injected up through the vertical 'fracture' at Source B. The lower enthalpy of fluid here reflects a slightly lower temperature that was observed in well SV-17.
- Source C, under the main well field in Svartsengi was modelled with a total mass flow rate of 105 kg/s, with an average enthalpy of 1060 kJ/kg total mass flow rate for the elements within the liquid dominated reservoir.
- Wells SV-02, SV-03 and SV-10 have been observed to lie in the two phase zone. In order to simulate the temperature in this zone, 10 kg/s of fluid, with an enthalpy of 1350 kJ/kg was applied. Additionally, in the first active layer of the model (Layer B), a 'safety valve' in the form of a productivity index (PI) of 3 x 10^{-13} m^3 and bottom well pressure of 35 bar was applied to the elements that make up the two-phase zone to simulate the release of steam and to maintain the boiling point curve with depth. A similar approach was taken by both Björnsson (1999) and Ketilsson (2007).

A vertical WSW-ENE trending cross section (X-X') extending from Eldvörp to Svartsengi (location depicted in Figure 10A) of the complete temperature model that incorporates each element generated by TOUGH2 was created using Leapfrog Geothermal and is presented in Figure 10B. Here we see that the modelled results replicate the isothermal temperatures of the main well field. The extrapolated downhole formation temperature and modelled well temperature profiles are presented in Figures 10C and 10D for comparison. Overall, they show fairly good correlation between modelled and measured temperature within the wells.

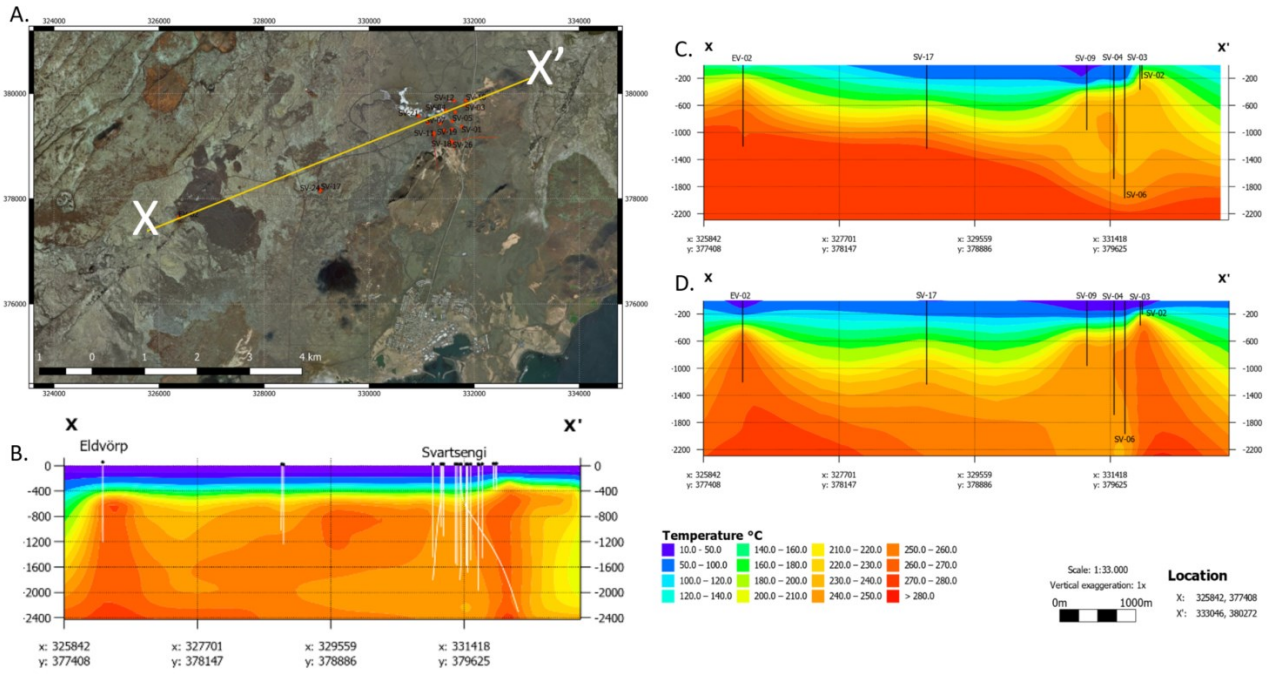

Figure 10: (A) Location of WSW-ENE trending temperature cross section showing (B) the natural state TOUGH2 temperature model of the Svartsengi reservoir, with a comparison between the downhole formation (C) and modelled (D) temperature profiles.

The modelled data, however, shows lower temperatures at the surface down to approximately 200 m b.s.l., which is due to the inactive constant temperature boundary condition applied to Layer A (0 - 200 m b.s.l.). In the model, higher temperatures peaks are observed close to the higher temperature wells EV-02 and SV-17. These however vary somewhat when compared to the downhole formation temperature profiles. In the model, the maximum temperatures in Layer F (-1050 m) recorded in wells EV-02 and SV-17 are 267 °C and 249 °C, respectively, as compared to 270°C and 245°C in the measured downhole temperature.

Wells SV-02, SV-03 are shallow wells, producing from the steam zone in the north east part of the field, temperature values below this depth are not known. The modelled temperature profile however simulates temperatures from sea-level to 2550 m b.s.l. The effects of higher enthalpy fluid that flows up the connection to this zone is one of the main discrepancies between the two profiles in Figure 39.

5.2 Production Response Model

The output from the temperature model was used as the initial conditions for the production response model. The modelled pressure was taken at 1050 m b.s.l. while the measured drawdown is observed at 900 m b.s.l. which accounts for a hydrostatic pressure difference of approximately 40 bars. The correlation graphs between the measured and modelled pressure response presented in Figure 11, show a fairly good correlation between measured and modelled drawdown, although underestimated by approximately 5-10 bars for the observation period 1985 to 2010. On observation, from the year 2000, after the onset of large scale reinjection,

whereas the pressure drawdown in the monitoring wells appear to be stabilising, the modelled response show less recovery than observed for this period in all monitoring wells.

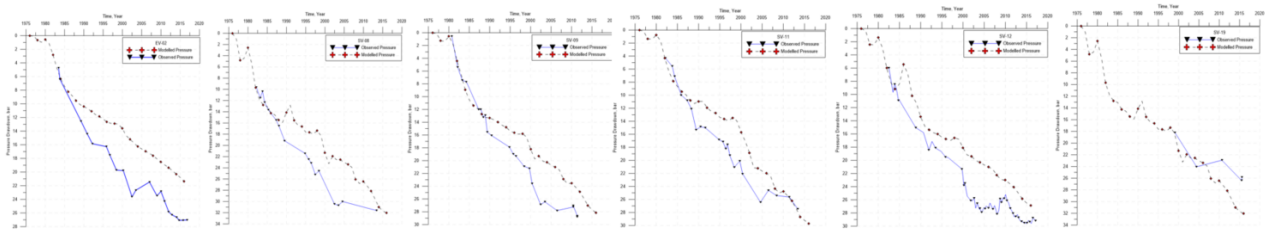

Figure 11: Comparison between observed and modelled pressure drawdown in wells EV-02, SV-08, SV-09, SV-11, SV-12 and SV-19.

Figure 12A shows a horizontal contour plot of the pressure drawdown at 900 m b.s.l. in a Leapfrog generated model from the TOUGH2 output. A pressure drawdown of between 25-30 bars is modelled around the main well-field at Svartsengi, with a maximum drawdown of approximately 32 bars observed around wells SV-07 and SV-08. Pressure recovery is observed around the reinjection site SV-17. The total average modelled pressure drawdown in the Svartsengi reservoir during 1975-2015 is 30 bars. From around 1987 to 2005 however, the modelled drawdown is approximately 5-10 bars lower than the measured drawdown which may be largely due to the high mass flow from the upflow source C under the main well field and two-phase zone, which may have provided excess pressure support to the model.

Model calibration was overall achieved by:

1. Modelling up-flow zones A, B and C as vertical fractures (FRAC1, FRAC2, and FRAC3) with high vertical permeabilities (Figure 35). Although Icelandic rocks typically have a porosity between 10-15%, these rock materials that were modelled as fractures were given higher permeabilities of 30%.
2. Inserting a narrow, high permeability zone extending from Eldvörp to Svartsengi (RCK06) and increasing the permeability of each layer from the boundary (BOUND) towards this high permeability zone (Figure 36) from Layers E-L. This reduced the pressure support from the reservoir boundaries, therefore increasing the pressure connection between Eldvörp and Svartsengi. This was done primarily because of the model's production response, to simulate pressure drawdown in Eldvörp.
3. Introducing a new rock type for the steam zone from Layer C to Layer E with average permeabilities of 290 mDarcy and 80 mDarcy in the horizontal and vertical directions respectively. In order to sustain a high enthalpy in these layers, a porosity of 60% was applied in order to simulate the higher steam enthalpy. This should be viewed as an artificial parameter selection, used to achieve the desired effect, without complicating the modelling process. This is justified by the fact that the focus of this study is not the steam zone, but rather the subsidence.

5.3 Subsidence

The subsidence module in iTOUGH2 was applied to the production model to calculate the changes in elevation of each element. These changes were integrated along the vertical column of each element. The overall elevation changes generated by iTOUGH2, with respect to the fixed 'inactive' TOUGH2 boundary for the period 1975 to 2015 is given in Figure 12B. Based on the model, with respect to the reservoir boundaries, the reservoir has subsided by an average of 100-200 mm during this period, with a maximum subsidence of 350 mm (0.35 m) in the steam zone. This is approximately equal to the maximum subsidence of 0.359 m observed in the main well field in 2015 (Magnússon, 2015).

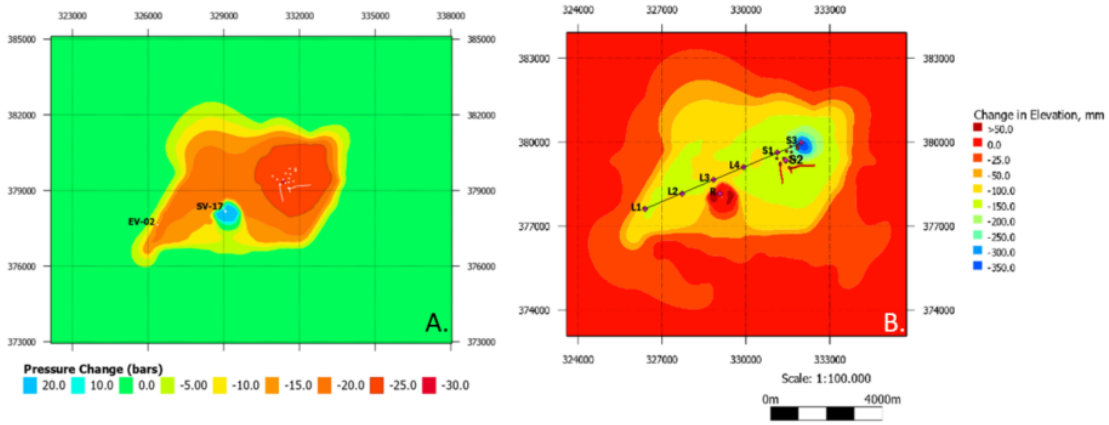

Figure 12: (A) Map showing pressure drawdown and (B) elevation changes in the Eldvorp-Svartsengi region during 40 years production (1975-2015)

The subsidence map is closely related to the modelled pressure drawdown for the same period. A profile was taken along the highly permeable region extending from Eldvörp to Svartsengi (location identified in Figure 12B). Annual modelled values of subsidence and pressure were selected for each point highlighted in Figure 12B from 1975-2015. Correlation graphs for points L1, L2, S2 and S3 are presented in Figure 12. They reveal a rather direct relationship between modelled drawdown and modelled subsidence along

the field from Eldvörp to Svartsengi, which is not unexpected. As pressure drawdown increases, this leads to a reduction in the pore pressure of surrounding reservoir rocks, thus creating a reduction in the rock matrix, and thereby subsiding. Point S3, which is located in the steam zone, however, shows slight deviation, which may imply that there is another causal factor responsible for subsidence, such as a decrease in temperature, which may be linked with the development of the steam zone. These results are in general agreement with observations during 1975 to 2010, although they deviate from the observed rate after 2008. With increased reinjection into SV-17 and SV-24, subsidence has been reported as being somewhat insignificant after 2010 (Magnússon, 2015). However, the modelled results show a slight increase in subsidence towards the main well field during 2010-2015.

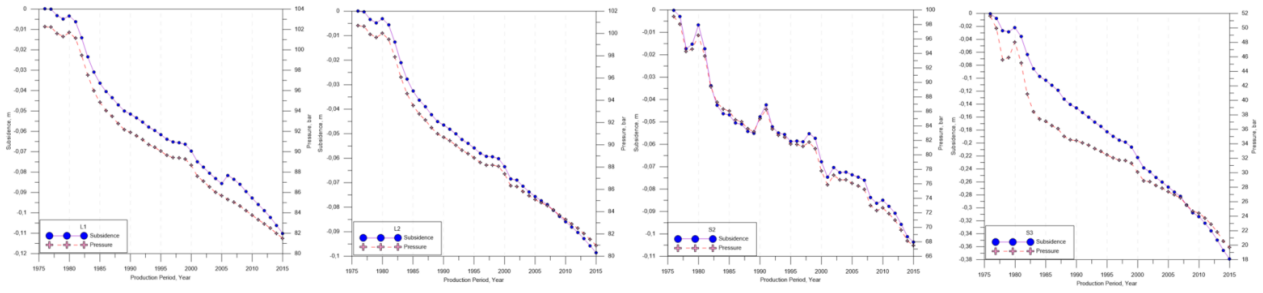

Figure 13: Comparison between modelled subsidence and pressure decline at points L1, L2, S2 and S3.

To investigate this further, the rate of change of subsidence and pressure with time were calculated for the periods 1975-1980; 1980-1985; 1985-1990; 1990-1995; 1995-2000; 2000-2005; 2005-2010; and 2010-2015. The highest subsidence at an average rate of 6-7 mm/year is observed during 1980-1985 throughout the field, with the steam zone subsiding at a rate of 16 mm/year. The subsidence rate decreased to an average of 2 mm/year during following years, after which it maintained a steady rate of approximately 3 mm/year until 2010. Pressure recovery and uplift (or reduction in the subsidence rate) is modelled on approaching the well field at the point S2 (Figure 13) during the periods 1989-1991, 1997-1998, 2000-2002, 2008-2010, which may be an effect of increased reinjection in SV-17 and SV-24 during this period.

The overall model reveals that pressure drawdown and changes in production and reinjection have played major roles in the vertical deformation at Svartsengi. For a more accurate comparison, subsidence at point S2, which is located in the same element as wells SV-07, SV-08 and SV-19, has been plotted alongside the pressure drawdown observed in well SV-08 (Figure 5B) from 1975-2015. These were compared with the average annual production and reinjection at Svartsengi from 1975-2015 and the results are presented in Figure 14.

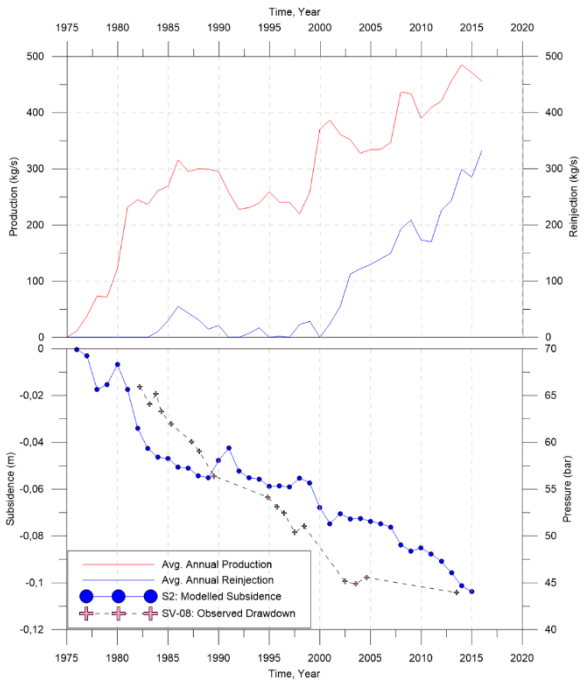

Figure 14: A graph showing the correlation of the annual average production and reinjection, on one hand, with observed pressure drawdown in well SV-08 and modelled subsidence at point S2, on the other hand.

Figure 14 reveals a close correlation between observed drawdown in well SV-08 and modelled subsidence at point S2 from 1982 to 2005. Observed drawdown in SV-08 exhibited a rapid decline of an estimated 10 bars during 1982-1989 correlating to high rates of both observed subsidence (Eysteinsson, 2000) and modelled subsidence during this period. A minor decrease in the modelled subsidence from 1991 to 1999 shows a relationship with a reduction in the pressure drawdown from 1990 to 1994. Modelled subsidence also appears to be affected by the reduced production, and the introduction of reinjection in the main well field around this period.

A considerable reduction in pressure drawdown has, however, been observed from since around 2002 as a response to the inception of reinjection of fluid into well SV-17 in 2000, despite an increase in the average annual production. The period (2000-2005) similarly experienced a reduction in both observed and modelled subsidence. The modelled subsidence however appears to deviate from observed after 2008 despite a large decrease in the net production, due to a large increase in the volume of fluid being injected into SV-17 and SV-24. The model, although it reacts well to early reinjection within the wellfield, deviates from expected, with a somewhat greater than expected modelled drawdown and subsidence.

A few years after production started, the area of maximum subsidence was observed at a point between Svartsengi and Eldvörp (Eysteinsson, 2000). This, however, was not reproduced in the model, with maximum subsidence occurring solely in the steam zone. This deviance may, however, be explained by a limited resolution or accuracy in the observed data due to the larger distances between elevation stations, whereas in the model, the subsidence was calculated for each element, which is a much denser network than what was measured in reality. Additionally, divergence from observed/expected values could have occurred due to an overestimation of volumetric strain in the z-direction. Since the subsidence module in iTOUGH2 only models one dimensional deformation, all deformation is assumed to be vertical, whereas in reality, some horizontal deformation will also occur.

Even though these factors are very likely to explain the modelled deviation, at least partly, another possible explanation could be changes due to seismicity as a result of recorded seismic events around this period. Approximately 82 earthquakes of magnitudes ranging between -0.9 to 1.9 ML were recorded around the reinjection wells, approximately 3 km WSW of the production field during December 2008 – May 2009, with epicentres located between 2 and 5 km depth (Guðnason 2014). A significant earthquake swarm with a total of 29 earthquakes occurred within a five hour period on March 6, 2009. It was centred approximately 500 m north-west of the injection boreholes at Svartsengi with magnitudes ranging from 0.17 ML to 1.26 ML (Guðnason 2014). In such cases, unexplained pressure recovery may occur despite stable production from the reservoir as was observed in Þykkvabær in 2000 (Björnsson, et al. 2001). This may explain the decrease in pressure drawdown observed in the Svartsengi well field in 2008. This seismic signal however is not included in this model.

6. CONCLUSIONS AND RECCOMMENDATIONS

The numerical model developed here only considers vertical deformation due to the mass production at Svartsengi, and ignores all other signals of deformation. Based on the results calculated by this model, the surface of the Eldvörp-Svartsengi geothermal field with reference to the reservoir boundary, is subsiding at an average rate of 3-4 mm/year during the production period 1975 to 2015. This value increases on approaching the steam zone where the modelled subsidence is greatest, at an average rate of 8-9 mm/year due to the expansion of the steam zone, where subsidence would be greater due to the higher compressibility of steam, as compared to that of liquid water and basaltic reservoir rocks.

Overall, there was a direct correlation between pressure drawdown, subsidence, and changes in production and reinjection. This when added to the natural rate of subsidence along the central volcanic rift of the Reykjanes Peninsula, represents the contribution of geothermal production to vertical crustal deformation at Svartsengi.

The simulations performed correlate well with the observed conditions in the Svartsengi geothermal system, despite observed deviations between both datasets. The following recommendations are proposed as further improvements:

1. Modelled parameters were manually adjusted throughout the development of the numerical model. In an effort to better estimate these parameters, inverse modelling with iTOUGH2 is recommended. With a better calibrated fit, the subsidence module can then be tested on a more complex model, such as Vatnaskil's existing reservoir model of the Svartsengi system.

2. Accuracy could be further improved by calibrating the model against mass changes observed as gravity changes due to mass extraction and reinjection. Gravity calibration is extremely useful in detecting the areal extent of boiling within the reservoir. This will serve as a further calibration tool for numerical modelling.

3. As a recommendation for future work in ground deformation studies at Svartsengi, a two or three-dimensional subsidence model can be set up to model the extent of the subsidence bowl that was created after the commencement of production in 1976. This can be done through the combined analysis of InSAR, geodetic modelling methods such as Mogi Modelling and reservoir modelling employing the Integral Finite Difference Method, thereby giving a more holistic view of the elevation changes along the Svartsengi Geothermal System.

Despite only considering one-dimensional subsidence, the model accurately simulates the subsidence observed at Svartsengi. The newly developed subsidence module in iTOUGH2 is therefore a valuable tool that can be used for predictions due to future geothermal production at Svartsengi and Eldvörp. The addition of subsidence data to reservoir models not only has the potential to increase its accuracy, but the direct correlation of subsidence and pressure makes it possible to calibrate the model in parts of the reservoir where there are no drawdown measurements, or no wells drilled.

ACKNOWLEDGEMENTS

The authors wish to thank HS Orka for allowing access to and granting permission to utilise and publish the Svartsengi data. Special thanks to Stefan Finsterle for allowing us to test your subsidence module, but also for personally taking the time to assist along the way. The authors would also like to express special thanks to Seequent Limited, for granting an academic license for Leapfrog Geothermal free of cost for the duration of this project.

REFERENCES

Árnadóttir, Þora, Halldór Geirsson, and Páll Einarsson. 2004. "Coseismic stress changes and crustal deformation on the Reykjanes Peninsula due to triggered earthquakes on 17 June 2000." *Journal or Geophysical Research* (109): 1-12.

Björnsson, G. 1999. "Predicting future performance of a shallow steam-zone in the Svartsengi." *Proceedings of the 24th Workshop on Geothermal Reservoir Engineering.* Stanford, CA: Stanford University. 7 pp.

Björnsson, Grímur, and Benedikt Steingrímsson. 1991. *Hiti og þrýstingur í jarðhitakerfinu í Svartsengi- Upphafsástand og breytingar vegna vinnslu.* Prepared for Hitaveitu Suðurnesja OS-91016/JHD-04, Reykjavík: Orkustofnun.

Björnsson, Grimur, Ólafur Flóvenz, Kristjan Sæmundsson, and Einar Einarsson. 2001. "Pressure changes in Icelandic geothermal reservoirs associated with two large earthquakes in June 2000." *Twenty-Sixth Workshop on Geothermal Reservoir Engineering.* Stanford: Stanford University.

Böðvarsson, G. S. 1988. "Model predictions of the Svartsengi reservoir, Iceland." *Water Resources Research* (12-10): 1740-1746.

Clifton, Amy E., and Simon A. Kattenhorn. 2006. "Structural architecture of a highly oblique divergent plate boundary segment." *Tectonophysics* (419): 27-40pp.

Croucher, Adrian. 2017. *PyTOUGH user's guide.* Auckland, New Zealand: University of Auckland.

De Freitas, Melissa Anne. 2018. *Numerical modelling of subsidence in geothermal reservoirs: Case study of the Svartsengi Geothermal System, SW Iceland.* Master´s Thesis, Faculty of Earth Science, Reykjavík: University of Iceland, 94 pp.

DeMets, C., R.G. Gordon, D.F. Argus, and S. Stein. 1994. "Effect of recent revisions to the geomagnetic reversal time scale on estimates of current plate motions." *Geophys. Res. Lett.* (21): 2191-2194pp.

Einarsson, Páll. 2008. "Plate boundaries, rifts and transforms in Iceland." *Jökull* (58): 35-58pp.

Eysteinsson, H. 2000. "Elevation and gravitational changes at geothermal fields on the Reykjanes Peninsula, SW-Iceland." *World Geothermal Congress WGC2000.* Kyushu-Tohoku, Japan. 559-564.

Eysteinsson, Hjálmar. 1993. *Hæðar- og þyngdarmælingar á utanverðum Reykjanesskaga 1992.* OS-93029/JHD-08, Reykjavík: Orkustofnun.

Finsterle, S. 2018a. *Enhancements to TOUGH2 simulator integrated in iTOUGH2. iTOUGH2, user manual.* Berkeley, CA: Lawrence Berkeley National Laboratory.

Finsterle, S. 2018b. *TOUGH2 v7.1.1 command reference. iTOUGH2 V7.1.1 manual.* Berkeley, CA: Lawrence Berkeley National Laboratory.

Franzson, Hjalti. 1987. "The Eldvörp high-temperature area, SW-Iceland. Geothermal geology of the first exploration well." *Proceedings of the 9th New Zealand Workshop.* 179-185pp.

Franzson, Hjalti. 1990. *Jarðfræðilíkan af háhitakerfi og umhverfi þess.* OS-90050/JHD-08, Reykjavík: Orkustofnun.

Franzson, Hjalti. 2017. *Svartsengi-Eldvörp: A conceptual geological model of the geothermal reservoir.* Closed Report ÍSOR-2017/017, Reykjavík: Iceland Geosurvey (ÍSOR).

Fridleifsson, G. Ó., and B. Richter. 2010. "The geological significance of two IDDP-ICDP spot cores." *Proceedings of the World Geothermal Congress WGC2010.* Bali, Indonesia. 7 pp.

Georgsson, Luðvík S. 1981. "A resistivity survey on the plate boundaries in the western Reykjanes Peninsula, Iceland." *Trans. Geothermal Resources Council* (5): 75-78pp.

Grant, Malcolm, and Paul Bixley. 2011. *Geothermal Reservoir Engineering.* 2nd Edition. New Yor: Academic Press.

Guðmundsdóttir, Valdís. 2016. *Svartsengi-Reykjanes reservoir temperature and pressure monitoring report 2015.* Closed Report ÍSOR-2016/032, Reykjavík: Iceland Geosurvey (ÍSOR).

Guðmundsson, J S. 1983. "Injection testing in 1982 at the Svartsengi high-temperature field in Iceland." *Trans. Geothermal Resources Council* (7): 423-428pp.

Guðnason, Egill Árni. 2014. *Analysis of seismic activity on the western part of the Reykjanes Peninsula, SW Iceland, December 2008 - May 2009.* Master´s Thesis, Reykjavík: University of Iceland.

Hreinsdóttir, S., P. Einarsson, and F. Sigmundsson. 2001. "Crustal deformation at the oblique spreading Reykjanes Peninsula, SW Iceland: GPS measurements from 1993-1998." *J. Geophy. Res.* 106 (B7): 13803-13816pp.

Karlsdóttir, Ragna. 1998. *TEM-viðnámsmælingar í Svartsengi 1997.* Closed Report, Reyjavík: Orkustofnun.

Karlsdottir, Ragna, and Arnar Már Vilhjálmsson. 2015. *Svartsengi-Eldvörp-Sandvík 3D Inversion of MT data.* Closed Report ÍSOR-2015/001, Reykjavík: Iceland Geosurvey (ÍSOR).

Keiding, Marie, Þóra Árnadóttir, E Sturkell, H Geirsson, and E Lund. 2008. "Strain accumulation along an oblique plate boundary: the Reykjanes Peninsula, southwest Iceland." *Geophysical Journal International* (172): 861-872pp.

Keiding, Marie, Þóra Árnadóttir, Sigurjón Jónsson, Andy Hooper, and Judicael Decriem. 2010. "Plate boundary deformation and man-made subsidence around geothermal fields on the Reykjanes Peninsula, Iceland." *Journal of Volcanology and Geothermal Research* (194): 139-149pp.

Ketilsson, J. 2007. *Production capacity assessment of geothermal resources by numerical modelling.* MSc thesis, Reykjavík: University of Iceland.

Kjaran, Snorri Páll, Gísli Karel Halldórsson, Sverrir Þórhallsson, and Jónas Elíasson. 1979. "Reservoir engineering aspects of Svartseni geothermal area." *Trans. Geothermal Resources Council* 3: 337-339pp.

Kjaran, Snorri Páll, Jónas Elíasson, and Gísli Karel Halldórsson. 1980. *Svartsengi- Athugun á vinnslu jarðhita.* Prepared for Hitaveitu Suðurnesja: OS080021/ROD10-JHD17, Reykjavík: Orkustofnun.

Koros, W., J. O´Sullivan, J. Pogacnik, and M. O´Sullivan. 2016. "Modelling of subsidence at the." *Proceedings of the 38th New Zealand Geothermal Workshop.* Auckland, New Zealand. 8 pp.

Magnússon, I. Þ. 2009. *GNSS- and gravity measurements on the outer Reykjanes Peninsula 2008.* report prepared for HS Orka Ltd, ÍSOR-2009/029 (in Icelandic), Reykjavík: ÍSOR- Iceland GeoSurvey, 60 pp.

Magnússon, I. Þ. 2013. *GNSS- and gravity measurements on the outer Reykjanes Peninsula 2010.* report prepared for HS Orka Ltd., ÍSOR 2013/066 (in Icelandic), Reykjavík: ÍSOR - Iceland GeoSurvey.

Magnússon, I. Þ. 2015. *GNSS- and gravity measurements on the outer Reykjanes Peninsula 2014.* report prepared for HS Orka Ltd., ÍSOR 2015/053 (in Icelandic), Reykjavík: ÍSOR - Iceland GeoSurvey.

Receveur, Mylene. 2018. *Ground deformation induced by geothermal utilization at Reykjanes, SW-Iceland, inferred from interferometric analysis of Sentinel-1 Synthetic Aperture Radar Images (InSAR).* MS Thesis, Reykjavík: University of Iceland.

Þóhallsson, S, T Hauksson , S P Kjaran, M Ólafsson, and A Albertsson. 2004. *Niðurdæling í Svartsengi frá tilraunum til stöðugs rekstrar.* Reykjavík: Málþing Jarðhitafélags Íslands.

Vadon, H., and F. Sigmundsson. 1997. "Crustal deformation from 1992 to 1995 at the Mid-Atlantic." *Science* (275): 193-197pp.

Wolfe, C.J., I.Þ. Bjarnason, J.C. Van Decar, and S.C. Solomon. 1997. "Seismic structure of the Iceland mantle plume." *Nature* (385): 245-247pp.